Title

LG_{01} Transverse LH Mode via Metamaterial Orbital Angular Momentum (OAM) Beam Generation

Author

Cervantes, Sebastian

Publication Date

2023-12-11

LG_{01} Transverse LH Mode via Metamaterial Orbital Angular Momentum (OAM) Beam Generation

Sebastian Cervantes

[1]*Undergraduate student majoring in Electrical Engineering at the University of California, Los Angeles*
scervantes47@g.ucla.edu

Abstract: Spiral phase plates are used to mitigate microbunching instability by generating an LG_{01} transverse laser mode[1]. Despite SPPs perks, such as their simple structure, metamaterials are another viable method of forming an LG_{01} mode.

INTRODUCTION

Free-electron lasers (FELs) commonly face microbunching instability (MBI), where collective effects induce an energy spread in the electron beam, degrading its quality. Laser heating (LH) using a Laguerre-Gauss (LG_{01}) transverse laser mode, generated by a spiral phase plate (SPP), was employed to mitigate MBI. While SPPs offer advantages, such as simplicity and precision, metamaterials present an alternative for forming LG_{01} transverse modes, leveraging orbital angular momentum (OAM) beams with a doughnut-shaped transverse mode. MBI attenuation, as discussed in Ref. [1], holds promise for various FEL operational modes, particularly in ultrafast x-ray spectroscopic techniques. As FELs become integral to societal technology, achieving MBI suppression requires a cost-effective method, making metamaterials a viable solution.

METHODS

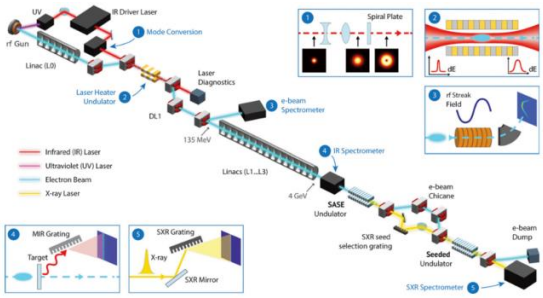

Figure 1. A simplified schematic of experimental set up: from LG_{01} formation to SXRSS (Ref. [1], Fig. 1).

The LG_{01} transverse mode was fashioned by the spiral phase plate: the SPP increments the phase of the beam for a total of 2π[1]. As a result, a null space is formed in the center of the field amplitude, generating a doughnut shaped transverse geometry figure 1 (inset 2). Due to the doughnut geometry of LG_{01}, the beam is placed in its center to apply a linear electric field; this causes a Gaussian transverse distribution of the electron beam[1].

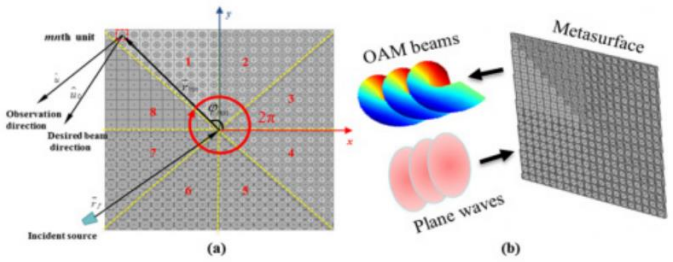

Figure 2. (a) Diagram of a metamaterial and its 8 sub-regions, causing an increasing phase shift of $\frac{\pi}{4}$. (b) depiction of OAM beam generation from plane waves and metasurface (Ref. [2], Fig. 3).

Alternatively, the LG01 transverse geometry can be generated through an OAM beam produced by a metamaterial. OAM beams exhibit a "corkscrew" vortex shape formed by the planes of constant phase of the electric and magnetic fields (Figure 2b). They are characterized by a topological charge representing the number of twists per wavelength. Metamaterials, illustrated in Figure 2a, are composed of sub-wavelength constituents like L-shape antennas, V-shaped antennas, or rectangular apertures, forming ultra-thin, planar optical components. When the beam interacts with the metamaterial, abrupt changes in amplitude, phase, or polarization induce a phase response accumulating up to 2π, akin to the SPP. The required phase shift for each element of the metasurface (a metamaterial rectangular plane) to radiate the beam in a desired direction can be determined using Equation 1[3].

$$\text{Equation 1: } {}^{\Phi c}_{mn} = l\varphi_{mn} + k_0[|\overrightarrow{r_{mn}} - \overrightarrow{r_f}| + \overrightarrow{r_{mn}} \cdot \widehat{u_0}] \quad l = 0, \pm 1, \pm 2, \ldots$$

Where, $\widehat{u_0}$ is the desired direction of radiation, $\overrightarrow{r_{mn}}$ is the position vector of the *mn* element of the metasurface, $\overrightarrow{r_f}$ is the position vector of the source, l is the desired OAM mode number, φ_{mn} is the azimuthal angle of the *mn*th element, k_0 is the propagation constant in vacuum, and ${}^{\Phi c}_{mn}$ is the required compensating phase of the *mn*th reflective element on the metasurface. One can change the phase in three ways: the desired direction $\widehat{u_0}$, the OAM mode number l, and the position of the feed source $\overrightarrow{r_f}$.

RESULTS AND INTERPRETATION

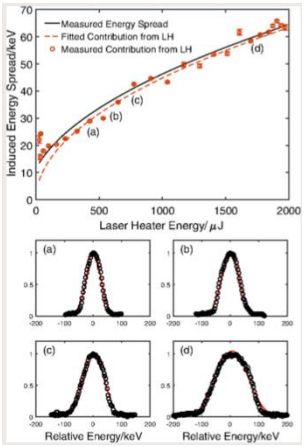

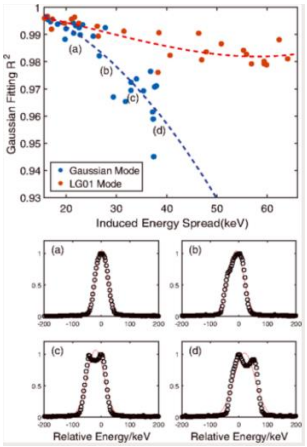

Figure 4. The total energy spread at 135 MeV spectrometer is illustrated by the black line in the plot. (a-d) show energy spreads at 25.1, 30.3, 36.8, and 55.7 keV, respectively (Ref. [1], Fig. 2).

Figure 5. R^2 for Gaussian fitting in relation to induced energy spread for both LG01 and Gaussian modes. (a)–(d) energy distributions from the transverse Gaussian mode with varying energy spreads (20.5, 26.7, 30.1, and 37.2 keV)(Ref. [1], Fig. 3).

To analyze the energy spread induced by the LG01 laser mode, the first diagnostic was immediately downstream of the LH using a 135 MeV spectrometer[1] (figure 1, inset 3). As illustrated in figure 4, the LG_{01} mode induced the desired Gaussian energy spread over a range of LH energies. Figure 5 also shows the inability of the Gaussian laser mode to induce Gaussian energy spreads (a double horn shape) as its energy increase, an issue that is absent for LG_{01}.

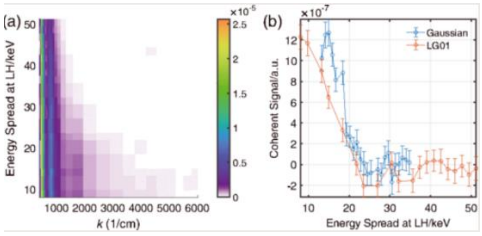

Figure 6. (a) 2D MIR spectrograph illustrating the induced energy spread by the LG01 transverse mode laser heater, and (b) integrated MIR spectral intensity for $k \in (3000, 5000)$ cm^{-1} depicting the induced energy spread by both LG01 and Gaussian mode laser heaters (Ref. [1], Fig. 4).

The second diagnostic was positioned past the linear accelerator, where a mid-infrared (MIR) spectrometer was used to assess the MBI through coherent secondary emission of the electron beam. In other words, the MIR measured the coherent transient radiation, which is directly proportional to the bunching factor of the beam. As seen in figure 6b, LG_{01} suppressed MBI in the range of 15-20 keV better than the Gaussian mode.

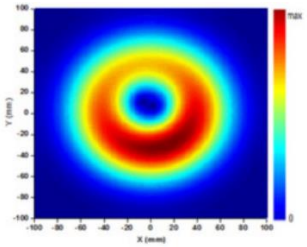

Figure 8. A simulated transverse profile with topological charge 1 (Ref. [2], Fig. 4a).

According to Ref. [2], a doughnut-shaped transverse profile was produced using an OAM beam and a metamaterial. The results, acquired at 10 GHz, revealed an intensity distribution shaped like a doughnut with a 2π phase change around the center, providing confirmation of OAM beam generation. The measured reflection spectra matched simulations, showcasing an 80% conversion efficiency. Both simulation and experimental data substantiate the effectiveness of reflective metasurfaces in generating OAM beams in the microwave domain. This suggests the possibility of achieving higher-order OAM modes through meticulous design modifications.

CONCLUSIONS

LG_{01} was experimentally shown to suppress MBI more than the Gaussian laser mode; this was seen in the energy distribution shape of both modes and their Gaussian fitting R^2 values across different laser heater energies. The key to inducing a Gaussian energy spread, and thus mitigating MBI, is the doughnut geometry of the LG_{01} transverse laser mode. Generating this

transverse geometry in laser heaters can be done in a number of ways, but metamaterials (specifically metasurfaces) are a path to be considered because of their easy integration, small size and price.

REFERENCES

1. Tang, J., Lemons, R., Liu, W., Vetter, S., Maxwell, T., Decker, F. J., ... & Carbajo, S. (2020). Laguerre-gaussian mode laser heater for microbunching instability suppression in free-electron lasers. *Physical review letters*, *124*(13), 134801.
2. Xu, B., Wu, C., Wei, Z., Fan, Y., & Li, H. (2016). Generating an orbital-angular-momentum beam with a metasurface of gradient reflective phase. *Optical materials express*, *6*(12), 3940-3945.
3. Yu, S., Li, L., Shi, G., Zhu, C., Zhou, X., & Shi, Y. (2016). Design, fabrication, and measurement of reflective metasurface for orbital angular momentum vortex wave in radio frequency domain. *Applied physics letters*, *108*(12).
4. Chen, R., Zhou, H., Moretti, M., Wang, X., & Li, J. (2019). Orbital angular momentum waves: Generation, detection, and emerging applications. *IEEE Communications Surveys & Tutorials*, *22*(2), 840-868.